Particulate Science and Technology: An International Journal
Publication details, including instructions for authors and subscription information:
http://www.tandfonline.com/loi/upst20

Promoting Photocatalytic Performance of ZnO Particles by Photochemically Reducing Ag^+ on the Particle Surfaces

Hsuan-Fu Yu[ab] & Dong-Wei Qian[a]
[a] Department of Chemical and Materials Engineering, Ceramic Materials Laboratory, Tamkang University, New Taipei City, Taiwan
[b] Energy and Opto-Electronic Materials Research Center, Tamkang University, New Taipei City, Taiwan
Accepted author version posted online: 02 Sep 2014.Published online: 02 Sep 2015.

To cite this article: Hsuan-Fu Yu & Dong-Wei Qian (2015) Promoting Photocatalytic Performance of ZnO Particles by Photochemically Reducing Ag^+ on the Particle Surfaces, Particulate Science and Technology: An International Journal, 33:2, 197-203, DOI: 10.1080/02726351.2014.948977

To link to this article: http://dx.doi.org/10.1080/02726351.2014.948977

Particulate Science and Technology, 33: 197–203

ISSN: 0272-6351 print/1548-0046 online
DOI: 10.1080/02726351.2014.948977

Taylor & Francis
Taylor & Francis Group

Promoting Photocatalytic Performance of ZnO Particles by Photochemically Reducing Ag^+ on the Particle Surfaces

HSUAN-FU YU[1,2] and DONG-WEI QIAN[1]

[1]*Department of Chemical and Materials Engineering, Ceramic Materials Laboratory, Tamkang University, New Taipei City, Taiwan*
[2]*Energy and Opto-Electronic Materials Research Center, Tamkang University, New Taipei City, Taiwan*

Dispersive Ag nanoparticles were formed on the surface of crystalline ZnO particles, using a photochemical reduction technique, to produce the Ag/ZnO with high photocatalytic performance. The prepared Ag/ZnO particles, as well as the ZnO particles without Ag attachments, were characterized using x-ray diffractometer, transmission electron microscope, and surface area analyzer. The abilities of the ZnO and the Ag/ZnO particles to photocatalytically decompose methylene blue under 365-nm ultraviolet light irradiation were evaluated by determining the corresponding specific reaction rate constant, $k'_{MB,m}$ (based on the mass of the photocatalyst used). While the ZnO crystalline particles ($k'_{MB,m} > 0.43\,m^3/(kg\ min)$) already possessed better photocatalytic performance than the commercial photocatalyst P25 ($k'_{MB,m} = 0.39\,m^3/(kg\ min)$), the Ag/ZnO particles exhibited much better photocatalytic performance than the ZnO particles. The highest $k'_{MB,m}$ for the Ag/ZnO particles was $1.93\,m^3/(kg\ min)$, which was about five times that of the P25.

Keywords: Ag deposition, photocatalysis, photochemical reduction, polyol method, zinc oxide

1. Introduction

ZnO with a hexagonal crystal structure is an n-type semiconductor material, which has a wide-bandgap energy of 3.37 eV and an exciton binding energy of 60 meV. Like TiO_2 (Hoffmann et al. 1995), ZnO is one of the most promising photocatalytic materials for purification and disinfection of water and air and remediation of hazardous waste, owing to its high activity, environment-friendly feature, and lower cost (Li and Haneda 2003a; Pauporte and Rathousky 2007; Sobana and Swaminathan 2007; Qiu et al. 2008). Photocatalytic ZnO particles have been synthesized by diverse methods, such as precipitation (Zhang and Li 2003; Wang et al. 2010), hydrothermal method (Musić et al. 2005; Lu et al. 2009; Lai et al. 2011), spray pyrolysis (Li and Haneda 2003b; El Hichou et al. 2005), and solid-state method (Lin and Li 2009; Estruga et al. 2010; Tian et al. 2012). Under ultraviolet (UV) light ($\lambda \leq 368$ nm) irradiation, the electron in the valence band of ZnO is excited to the conduction band, and the hole with positive charge is simultaneously generated in the valence band of ZnO. These photoinduced electron-and-hole pairs can react with the oxygen and the surface hydroxyl to ultimately produce strong oxidizing substances, the hydroxyl radicals (·OH). These hydroxyl radicals are capable of decomposing many of organics and are responsible to the photocatalysis of ZnO. On the other hand, the photoinduced electrons and holes will recombine with each other, resulting in abating the photocatalytic ability of ZnO. To reduce the negative effect from the recombination of the photoinduced electrons and holes on the photocatalysis of ZnO, one of the approaches extensively used is to couple ZnO with the substance that acts as an electron sink to eliminate or slow down the recombination process of photoinduced electrons and holes. Several materials, like Ag (Georgekutty et al. 2008; Ren et al. 2010; Tian et al. 2010; Aguirre et al. 2011; Yin et al. 2012; Wu et al. 2014), SnO_2 (Shi et al. 2000; Cun et al. 2002; Zheng 2009), Cu_2O (Xu 2010), and C (Yu and Chou 2013), were used as electron sink to enhance the photocatalytic ability of ZnO.

In this study, a facile two-step process combining the polyol method and the photochemical reduction technique was used to prepare the ZnO photocatalytic particles coupled with dispersive Ag nanoparticles (Ag/ZnO). Characteristics and photocatalytic activities of the ZnO particles with or without the attachment of Ag, as well as the P25 (a commercial TiO_2 photocatalyst product; Degussa, Germany), were measured, and the results were compared with each other. Effects of the Ag^+ concentration and the ZnO calcination temperature used in preparation on the photocatalytic performance of the obtained Ag/ZnO were systematically studied.

Address correspondence to: Hsuan-Fu Yu, Department of Chemical and Materials Engineering, Ceramic Materials Laboratory, Tamkang University, New Taipei City 25137, Taiwan. E-mail: hfyu@mail.tku.edu.tw

Color versions of one or more of the figures in the article can be found online at www.tandfonline.com/upst.

2. Experimental Detail

2.1 Sample Preparation

The crystalline ZnO particles were prepared using a polyol method. $Zn(NO_3)_2 \cdot 6H_2O$ (99% purity, Showa, Tokyo, Japan) was dissolved in ethylene glycol ($C_2H_4(OH)_2$; 99.5% purity, Echo) to form a transparent solution of 0.2 M. The solution so obtained, with continuously stirring, was heated up to 160°C in a glass reactor with reflux, followed by isothermal heating for 8 h. After reaction and cooling, the resultant suspension was centrifugally filtered, washed with distilled water twice, and then dried in an oven at 90°C. The dried precursors were calcined in a muffle furnace at temperature T (=400°C, 500°C, 600°C, or 700°C) for 3 h to form crystalline ZnO particles.

The photochemical reduction technique was used to deposit Ag nanoparticles on the surface of the calcined ZnO particles. About 0.5 g of the crystalline ZnO particles calcined at T was uniformly dispersed in stirred 150-mL distilled water. The suspended particles were irradiated by the 254-nm UV light (8 W × 4, Philips, Pila, Poland) for 1 h. The suspended ZnO particles were excited by the UV light, forming electron–hole pairs in the particles. Then, 50-mL aqueous solution containing proper amount of $AgNO_3$ (99.8% purity, Hwang Long, Tainan, Taiwan) was added to the suspension with continuously stirring, and the resultant suspension was again under the 254-nm UV light irradiation for another 1 h. Ag^+ around the ZnO particles was attracted by the photoexcited electrons and converted to metallic Ag on the surface of ZnO particles. The obtained Ag/ZnO particles were centrifugally filtered and dried in vacuum at 40°C. The amount of $AgNO_3$ used during preparation was controlled at R (a molar ratio in percentage of the $AgNO_3$ to the calcined ZnO used). Six different R (=0%, 1.5%, 2.5%, 3.5%, 4.5%, and 5%) were used to prepare the Ag/ZnO particles. The Ag/ZnO particles so obtained will be represented as Ag/ZnO [R/T].

2.2 Characterization

The crystalline phases and crystal structure existing in the Ag/ZnO [R/T] specimens were examined using an x-ray diffractometer (XRD; x-ray wavelength 0.154056 nm; D8A, Bruker, Karlsruhe, Germany). The average sizes of ZnO crystallites in Ag/ZnO [R/T] were estimated by employing Scherrer's equation in the corresponding profiles of the (101) XRD peak for ZnO. Morphologies and sizes of the crystallites were observed using transmission electron microscopy (TEM; H-7100, Hitachi, Tokyo, Japan). Specific surface areas of the specimens were measured using an automated BET sorptometer (Porous Materials, Ithaca, NY, USA), operated at a liquid-nitrogen temperature of around −196°C.

2.3 Photocatalytic Activity Determination

Photocatalytic activities of the prepared Ag/ZnO [R/T] and the P25 were estimated by examining their abilities to photocatalytically decompose the methylene blue (MB; $C_{16}H_{18}N_3SCl$) in water. The tested particles of 0.04 g were dispersed in an aqueous solution of MB (10 μM, 200 mL). The resultant suspension was vigorously stirred in a dark chamber for 10 min to attain the adsorption–desorption equilibrium of MB on the tested particles, which was confirmed by observing the change of concentration of the $MB_{(aq)}$ using an UV-visible spectroscope (UV-vis; EVO300PC, Thermo, Waltham, MA, USA). Then, the 365-nm UV lamps (8 W × 2, Philips) were turn on to trigger the photocatalytic degradation of MB. The reaction system was maintained at about 25°C. After every 5- or 10-min UV exposure, 3 mL of the testing MB solution was sampled and was subjected to UV-vis analysis. The absorbance of the MB characteristic band at 664 nm in the obtained UV-vis spectrum was used to determine the concentration of MB (C_{MB}) in the solution. The change in molar fraction of $MB_{(aq)}$ (C_{MB}/C_{MBo}; C_{MBo}: the initial concentration of $MB_{(aq)}$) with time (t) under the conditions described above were recorded and examined to determine the photocatalytic activities of the prepared nanoparticles.

To intrinsically reveal the abilities of photocatalysts to decompose MB, the corresponding specific reaction rate constant $k'_{MB,m}$ (based on the mass of the catalyst used) was estimated and examined. Since the changes of C_{MB}/C_{MBo} with t for all the tests obeyed Equation (1) (which will be shown in the next section), the apparent reaction order for photocatalytic decomposition of MB was considered as 1, and then $k'_{MB,m}$ was estimated using Equation (2) (Yu 2007), where A is the corresponding characteristic constant, V is the volume of the reaction liquid, and m is the mass of the photocatalyst used.

$$\frac{C_{MB}}{C_{MBo}} = e^{-At} \tag{1}$$

$$k'_{MB,m} = A\left(\frac{V}{m}\right) \tag{2}$$

3. Results and Discussion

3.1 Powder Characterization

All of Ag/ZnO [R/T] were XRD analyzed, and Figure 1 gives some of these XRD patterns. The dried precursor obtained from the polyol method transferred to crystalline ZnO (PDF # 36-1451) after being calcined at 400°C (see Figure 1(a)) or above. Raising the calcination temperature sharpened the XRD peaks of ZnO, indicating the increase in crystallinity of ZnO (or the increase in size of ZnO crystallites). Except for Ag/ZnO [1.5%/400°C] (Figure 1(b)), the (111) XRD peak of metallic Ag (PDF #89-3722) was detected in all of Ag/ZnO [$R \neq 0\%/400$–700°C] (e.g., Figure 1(c)–(f)). By examining the full widths at half maximum of the (111) XRD peak of Ag ($2\theta = 38.12°$) and the ratios of the integrated intensity of the (111) XRD peak of Ag to that of the (101) XRD peak of ZnO ($2\theta = 36.28°$), it was found that the crystallite size and the amount of Ag in Ag/ZnO increased with increasing R and/or T. Under UV light irradiation, the ZnO obtained at higher calcination temperature (i.e., higher T), which possesses higher crystallinity, can generate more photoexcited electrons on the

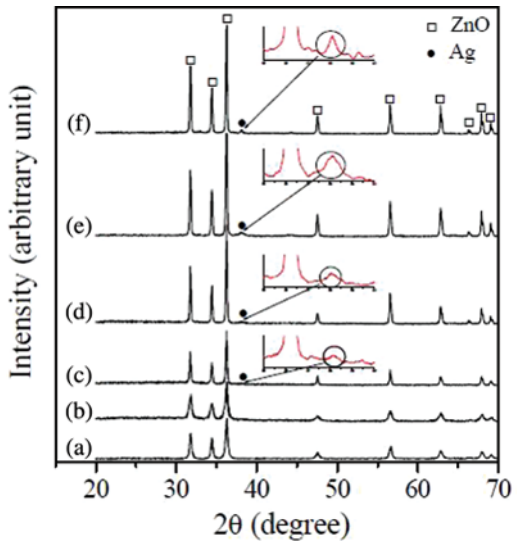

Fig. 1. XRD patterns of the specimen: (a) Ag/ZnO [0%/400°C], (b) Ag/ZnO [1.5%/400°C], (c) Ag/ZnO [1.5%/600°C], (d) Ag/ZnO [1.5%/700°C], (e) Ag/ZnO [3.5%/700°C], and (f) Ag/ZnO [4.5%/700°C].

surface of ZnO particles, and the $AgNO_{3(aq)}$ with higher concentration (i.e., higher R) can provide more Ag^+ around the ZnO particles. The ZnO particles calcined at higher temperature dispersed in the $AgNO_{3(aq)}$ with higher concentration leading to the formation of bigger sizes and more amounts of Ag crystallites on the ZnO particles. The absence of XRD peaks of Ag in Ag/ZnO [1.5%/400°C] should be due to the smaller size and the less amount of Ag attached on the surface of ZnO particles. It is to be noted that the color of the prepared particles was white for Ag/ZnO [0%/T] (i.e., no Ag deposition) but turned to light-gray after Ag deposition (i.e., for all of Ag/ZnO [$R \neq 0/T$]).

Figure 2 shows the average sizes of ZnO crystallites in Ag/ZnO [R/T]. Without Ag deposition (i.e., $R = 0\%$), the ZnO crystallites increased in size but decreased in specific surface areas (see the values in the parentheses in Figure 2) as T increased. After photochemically reducing Ag^+ on the surface of ZnO crystallites, the crystallite sizes of the calcined ZnO slightly decreased. This small size reduction of ZnO crystallites should be ascribed to slight corrosion of the ZnO in an acid solution. Figure 3 shows TEM images of the Ag/ZnO [R/500°C], where $R = 0\%$, 2.5%, 3.5%, and 4.5%. It is clear that after the photochemical reduction process, the scattered Ag nanoparticles were formed on the surfaces of ZnO crystallites. The sizes and amounts of these Ag nanoparticles increased with increasing concentration of the $AgNO_{3(aq)}$ used, which was in agreement with the results obtained from the XRD analysis. To examine the effect of Ag deposition on the specific surface area of ZnO particles, the specific surface areas (S_{BET}) of Ag/ZnO [R/500°C] were measured and shown in Figure 4. The values of S_{BET} for Ag/ZnO [$R = 0$ - 5%/500°C] were close to each other and had a mean specific surface area of $13.24 \pm 0.69\ m^2/g$, indicating that the effect of Ag deposition on specific surface areas of the Ag/ZnO [R/T] is negligible.

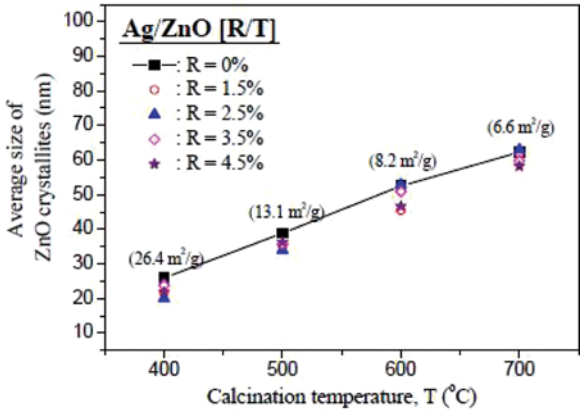

Fig. 2. Average sizes of ZnO crystallites in the various Ag/ZnO [R/T] specimens (the values in the parentheses are the specific surface areas of the Ag/ZnO [0%/T]).

3.2 Photocatalytic Abilities

Photocatalytic activities of the Ag/ZnO [R/T] were estimated by examining the ability of the particles to photocatalytically decompose the MB in water. Under 365-nm UV light irradiation, C_{MB}/C_{MBo} decayed exponentially with reaction time t for all of the Ag/ZnO [R/T] used and can be well described by Equation (1). Figure 5, for example, shows the variations of C_{MB}/C_{MBo} with t by using some of the Ag/ZnO [R/T] particles. It is evident that the apparent reaction order of the photocatalytic decomposition of MB by the prepared Ag/ZnO particles can be considered as 1. By plugging V ($=2 \times 10^{-4}\ m^3$), m ($=4 \times 10^{-5}$ kg), and the corresponding A (determined by fitting the MB concentration data to Equation (1)) into Equation (2), $k'_{MB,m}$ of the Ag/ZnO [R/T] were evaluated.

Figure 6 gives the estimated $k'_{MB,m}$ of Ag/ZnO [R/T] and P25. Without Ag deposition, the calcined ZnO particles prepared by the polyol process (i.e., Ag/ZnO [0%/T]) already possessed higher photocatalytic abilities than that of P25 ($k'_{MB,m} = 0.39\ m^3/(kg\ min)$). The $k'_{MB,m}$ of ZnO (or Ag/ZnO [0%/T]) increased with T till 500°C and then decreased with further increase in the calcination temperature. At $R = 0\%$, the ZnO calcined at 500°C exhibited the best photocatalytic performance, and its $k'_{MB,m}$ was $0.63\ m^3/(kg\ min)$, which was about 62% greater than that of P25. After Ag deposition, the photocatalytic abilities of the calcined ZnO were greatly enhanced. At $0 < R \leq 3.5\%$, the effects of T on photocatalytic abilities of the Ag/ZnO were similar to those of the ZnO (i.e., $R = 0\%$), which gave the highest $k'_{MB,m}$ at $T = 500$°C. However, at $R > 3.5\%$, the best photocatalytic performance of Ag/ZnO occurred at $T = 600$°C. The Ag/ZnO particles prepared at $R = 4.5\%$ and $T = 600$°C possessed the highest $k'_{MB,m}$ ($=1.93\ m^3/(kg\ min)$), which was about three and five times of those of Ag/ZnO [0%/500°C] and P25, respectively.

The performance of photocatalytic powder was governed by three major factors: the surface area, the crystallinity, and the recombination rate of photoinduced electron-and-hole pairs of the photocatalyst. The photocatalysts with high

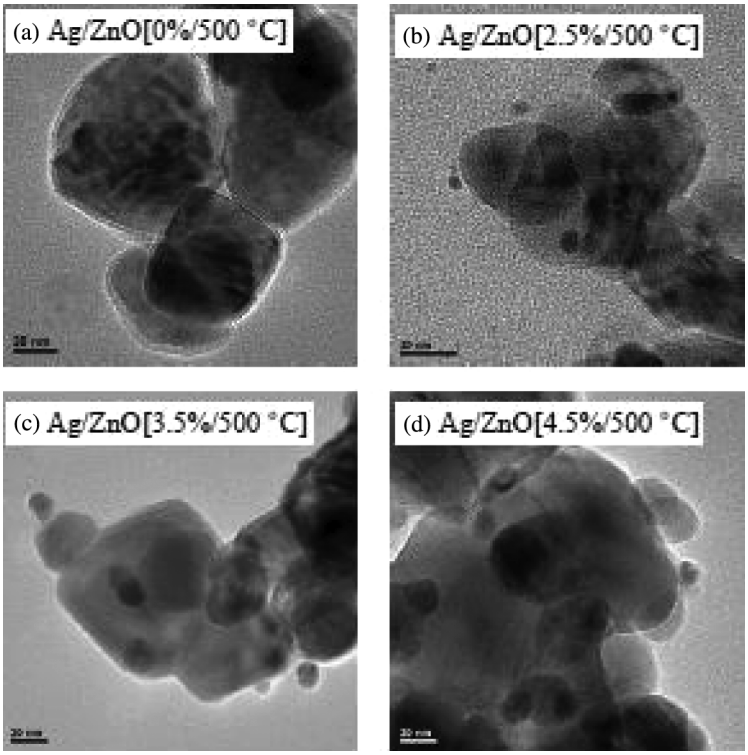

Fig. 3. TEM images of some selected Ag/ZnO [R/T] particles.

surface area, high crystallinity, or low recombination rate of the photoinduced electron-and-hole pairs usually possess high photocatalytic performance. Increasing the calcination temperature increases the crystallinity of ZnO but decreases the surface area of the particles (due to the increase of crystallite size and degree of particle agglomeration). On the other hand, Ag nanoparticles attaching to ZnO crystallites can partly transfer the photoexcited electrons from ZnO to Ag, which should hinder the recombination of electrons and holes in ZnO and result in more active sites existing on the surface of ZnO particles to undergo photocatalysis. However, higher amounts or bigger sizes of Ag nanoparticles on the surface of ZnO particles will also sacrifice more surface area of the ZnO powder to directly contact with the pollutant to undergo photocatalysis, which may curtail the positive effect of Ag deposition on the photocatalytic performance of Ag/ZnO.

By examining the variations of crystallite sizes (see Figure 2) and $k'_{MB,m}$ (see Figure 6) of Ag/ZnO [0%/T] with T, it can be found that the photocatalytic performance of the ZnO, without Ag deposition, was affected dominantly by the degree of crystallinity at $T \leq 500°C$ but by the surface area at

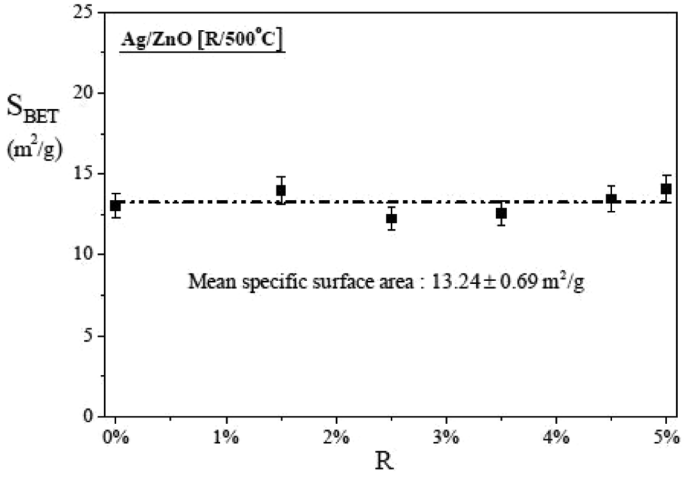

Fig. 4. BET-specific surface areas (S_{BET}) of Ag/ZnO [R/500°C].

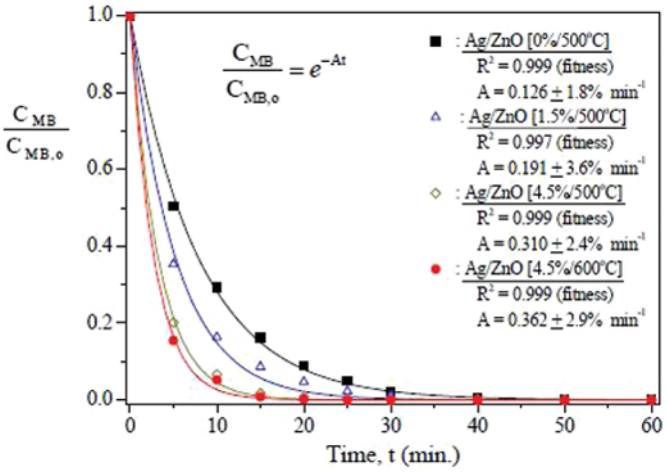

Fig. 5. Concentration changes of the $MB_{(aq)}$ with reaction time (t) during photocatalytic decomposition, under 365-nm UV light irradiation, using the photocatalysts of Ag/ZnO [R/T].

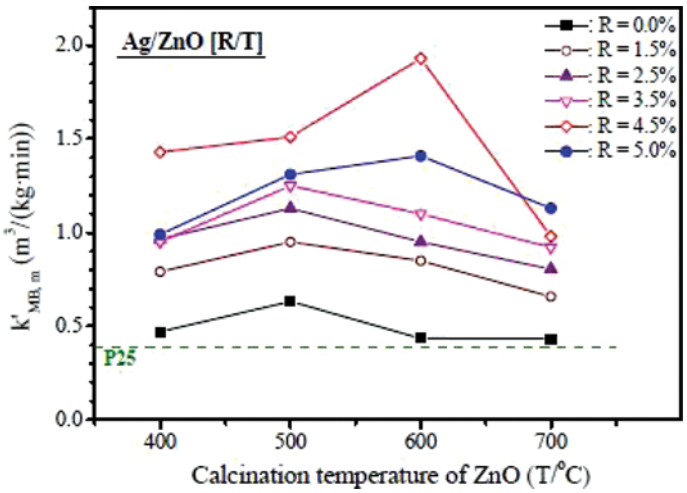

Fig. 6. $k'_{MB,m}$ of Ag/ZnO [R/T] and P25.

$T > 500$°C. After Ag deposition, the photocatalytic abilities of ZnO were greatly enhanced, as demonstrated in Figure 6. To quantitatively discover the effect of Ag deposition on the photocatalytic performance of the ZnO particles, the effectiveness (E) of Ag deposition at various R and T to promote photocatalytic ability of ZnO was estimated. E at R and T is defined as

$$\mathrm{E(R,T)} \equiv \frac{k'_{\mathrm{MB,m}} \text{ for Ag/ZnO } [R/T]}{k'_{\mathrm{MB,m}} \text{ for Ag/ZnO } [0\%/T]} \qquad (3)$$

Figure 7 shows E for the Ag/ZnO prepared at different R and T, as well as $k'_{MB,m}$ for Ag/ZnO [0%/T] as reference. At all T, the values of E for Ag/ZnO [$R \neq 0/T$] were higher than 1, revealing that the photocatalytic abilities of ZnO were promoted after dispersive Ag nanoparticles were deposited on the surface of ZnO particles. Ag nanoparticles attaching to the surfaces of ZnO particles can effectively capture the photoexcited electrons and then slow down the recombination rates of photoinduced electrons-and-holes of the ZnO, resulting in the enhancement of the photocatalytic ability of ZnO. Ag deposition achieved the maximum effectiveness in Ag/ZnO [4.5%/600°C], having its $E = 4.4$. Because this high E overturned the negative impact of the specific surface reduction (due to the increase of calcination temperature) on the photocatalytic performance of ZnO particles, the Ag/ZnO prepared at $R = 4.5\%$ possessed the highest $k'_{MB,m}$ at $T = 600$°C.

To examine if the Ag nanoparticles could be secured on the surface of ZnO particles and to measure the ease of reusing the catalyst, the recycling tests for photocatalytic performance of Ag/ZnO and P25 were conducted. After each photocatalytic test, the catalyst was recollected by centrifugation (6500 rpm for 30 min) and then re-dispersed in the $MB_{(aq)}$ for next recycling test. Figure 8 shows the molar percentages of the MB removed, after irradiating 365-nm UV light for 20 min, by Ag/ZnO [4.5%/600°C] and P25 in each recycling test. The photocatalytic performance of the recycled Ag/ZnO [4.5%/600°C] was similar to that of the fresh one, and the differences in the molar percentages of the MB removed between all these tests were less than 2%. The XRD analysis on the recycled Ag/ZnO [4.5%/600°C] showed that the crystalline phases and crystallite sizes of Ag/ZnO do not change after the recycling tests. All of these results implied that the Ag nanoparticles in Ag/ZnO are firmly attached to the surfaces of ZnO particles and the chemical phases in Ag/ZnO are stable. For P25, the amount of MB removed were slightly but continuously decreased with increasing the number of recycling test, which is mainly due to the difficulty to completely recollect the P25 particles (Tian et al. 2010). The P25 particles have very good dispersion in water and cannot be completely separated from the liquid using centrifugation at 6500 rpm for 30 min, resulting in the loss of P25 and consequently the

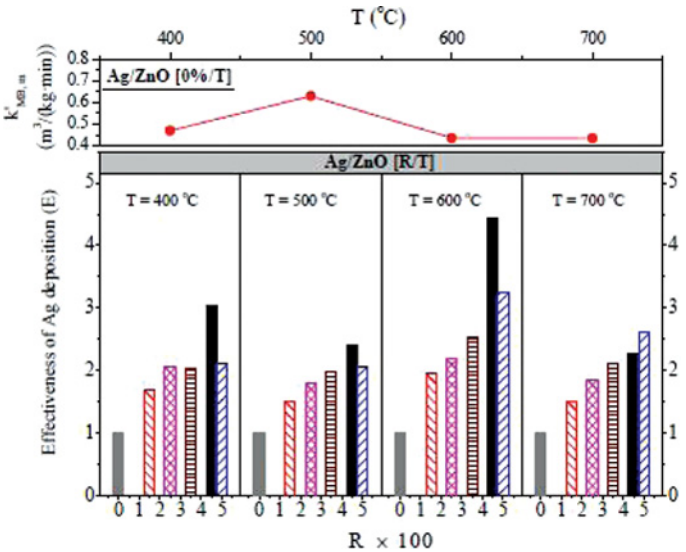

Fig. 7. Effectiveness of Ag deposition (E) for Ag/ZnO [R/T] and $k'_{MB,m}$ for Ag/ZnO [0%/T].

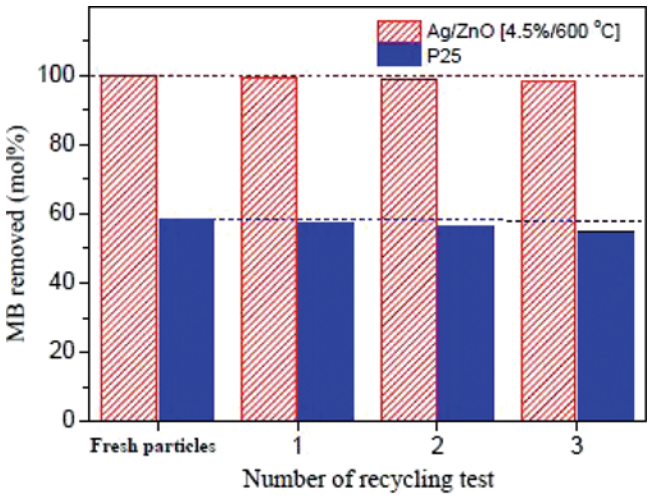

Fig. 8. MB removed percentages by the recycled Ag/ZnO [4.5%/600°C] and P25 particles, after irradiating 365-nm UV light for 20 min.

deterioration of photocatalytic performance in recycling test. Unlike P25, the Ag/ZnO particles, due to their dense structure, large sizes, and higher density, are easy to separate for reutilization.

4. Conclusions

The Ag/ZnO particles with high photocatalytic performance were prepared by a process combining the polyol method and the photochemical reduction technique. Without Ag deposition, the photocatalytic ability of the ZnO was affected dominantly by the degree of crystallinity at calcination temperature $T \leq 500°C$ but by the surface area at $T > 500°C$. The best photocatalytic performance of the ZnO without Ag deposition was the one calcined at 500°C, having its $k'_{MB,m} = 0.63\,m^3/(kg\ min)$. $k'_{MB,m}$ of Ag/ZnO [0%/500°C] was about 62% higher than that of the P25 ($k'_{MB,m} = 0.39\,m^3/(kg\ min)$). After Ag deposition, the obtained Ag/ZnO particles exhibited much higher photocatalytic ability than the ZnO particles. The amounts and crystallite sizes of the Ag nanoparticles attaching to the surfaces of ZnO particles were influenced by the calcination temperature of ZnO and the concentration of $AgNO_{3(aq)}$ used. The ZnO with higher crystallinity and/or the $AgNO_{3(aq)}$ with higher concentration led to the formation of bigger sizes or higher amounts of Ag nanoparticles on the surface of ZnO particles. While the polyol-derived crystalline ZnO particles already possessed the photocatalytic abilities ($k'_{MB,m} > 0.43\,m^3/(kg\ min)$) higher than the P25, Ag deposition retarded the recombination of photoinduced electrons and holes and further enhanced the photocatalytic performance of the ZnO. Ag/ZnO [4.5%/600°C] exhibited the maximum Ag deposition effectiveness ($E = 4.4$) and showed the highest photocatalytic ability ($k'_{MB,m} = 1.93\,m^3/(kg\ min)$). $k'_{MB,m}$ of Ag/ZnO [4.5%/600°C] was about three and five times that of the Ag/ZnO [0%/500°C] and P25, respectively.

References

Aguirre, M. E., H. B. Rodríguez, E. S. Román, A. Feldhoff, and M. A. Grela. 2011. Ag@ZnO core_shell nanoparticles formed by the timely reduction of Ag^+ ions and zinc acetate hydrolysis in N, N-dimethylformamide: Mechanism of growth and photocatalytic properties. *Journal of Physical Chemistry* C 115:24967–24974.

Cun, W., Z. Jincai, W. Xinming, M. Bixian, S. Guoying, P. Ping'an, and F. Jiamo. 2002. Preparation, characterization and photocatalytic activity of nano-sized ZnO/SnO_2 coupled photocatalysts. *Applied Catalysis B: Environmental* 39:269–279.

El Hichou, A., M. Addou, J. Ebothé, and M. Troyon. 2005. Influence of deposition temperature (Ts), air flow rate (f) and precursors on cathodoluminescence properties of ZnO thin films prepared by spray pyrolysis. *Journal of Luminescence* 113:183–190.

Estruga, M., C. Domingo, and J. A. Ayllón. 2010. Mild synthetic routes to high-surface zinc oxide nanopowders. *European Journal of Inorganic Chemistry* 11:1649–1654.

Georgekutty, R., M. K. Seery, and S. C. Pillai. 2008. A highly efficient Ag-ZnO photocatalyst: synthesis, properties, and mechanism. *Journal of Physical Chemistry* C 112:13563–13570.

Hoffmann, M. R., S. T. Martin, W. Choi, and D. W. Bahnemann. 1995. Environmental Applications of Semiconductor Photocatalysis. *Chemical Reviews* 95: 69–96.

Lai, Y., M. Meng, Y. Yu, X. Wang, and T. Ding. 2011. Photoluminescence and photocatalysis of the flower-like nano-ZnO photocatalysts prepared by a facile hydrothermal method with or without ultrasonic assistance. *Applied Catalysis B: Environmental* 105: 335–345.

Li, D., and H. Haneda. 2003a. Morphologies of zinc oxide particles and their effects on photocatalysis. *Chemosphere* 51:129–137.

Li, D., and H. Haneda. 2003b. Synthesis of nitrogen-containing ZnO powders by spray pyrolysis and their visible-light photocatalysis in gas-phase acetaldehyde decomposition. *Journal of Photochemistry and Photobiology A: Chemistry* 155:171–178.

Lin, C.-C., and Y.-Y. Li. 2009. Synthesis of ZnO nanowires by thermal decomposition of zinc acetate dehydrate. *Materials Chemistry and Physics* 113:334–337.

Lu, C.-H., Y.-C. Lai, and R. B. Kale. 2009. Influence of alkaline sources on the structural and morphological properties of hydrothermally derived zinc oxide powders. *Journal of Alloys and Compounds* 477:523–528.

Musić, S., D. Dragcević, S. Popović, and M. Ivanda. 2005. Precipitation of ZnO particles and their properties. *Materials Letters* 59:2388–2393.

Pauporte, T., and J. Rathousky. 2007. Electrodeposited mesoporous ZnO thin films as efficient photocatalysts for the degradation of dye pollutants. *Journal of Physical Chemistry C* 111: 7639–7644.

Qiu, X., L. Li, J. Zheng, J. Liu, X. Sun, and G. Li. 2008. Origin of the enhanced photocatalytic activities of semiconductors: a case study of ZnO doped with Mg^{2+}. *Journal of Physical Chemistry C* 112:12242–12248.

Ren, C., B. Yang, M. Wu, J. Xu, Z. Fu, Y. Iv, T. Guo, Y. Zhao, and C. Zhu. 2010. Synthesis of Ag/ZnO nanorods array with enhanced photocatalytic performance. *Journal of Hazardous Materials* 182:123–129.

Shi, L., C. Li, H. Gu, and D. Fang. 2000. Morphology and properties of ultrafine SnO_2-TiO_2 coupled semiconductor particles. *Materials Chemistry and Physics* 62:62–67.

Sobana, N., and M. Swaminathan. 2007. The effect of operational parameters on the photocatalytic degradation of acid red 18 by ZnO. *Separation and Purification Technology* 56:101–107.

Tian, C., W. Li, K. Pan, Q. Zhang, G. Tian, W. Zhou, and H. Fu. 2010. One pot synthesis of Ag nanoparticle modified ZnO microspheres in ethylene glycol medium and their enhanced photocatalytic performance. *Journal of Solid State Chemistry* 183:2720–2725.

Tian, C., Q. Zhang, A. Wu, M. Jiang, Z. Liang, B. Jiang, and H. Fu. 2012. Cost-effective large-scale synthesis of ZnO photocatalyst with excellent performance for dye photodegradation. *Chemical Communications* 48:2858–2860.

Wang, Y., C. Zhang, S. Bi, and G. Luo. 2010. Preparation of ZnO nanoparticles using the direct precipitation method in a membrane dispersion micro-structured reactor. *Powder Technology* 202: 130–136.

Wu, A., C. Tian, H. Yan, Y. Hong, B. Jiang, and H. Fu. 2014. Intermittent microwave heating-promoted rapid fabrication of sheet-like Ag assemblies and small-fabrication of sheet-like Ag assemblies and small-sized Ag particles and their use as co-catalyst of ZnO for enhanced photocatalysis. *Journal of Materials Chemistry A* 2:3015–3023.

Xu, C., L. Cao, G. Su, W. Liu, H. Liu, Y. Yu, and X. Qu. 2010. Preparation of ZnO/Cu_2O compound photocatalyst and application in treating organic dyes. *Journal of Hazardous Materials* 176:807–813.

Yin, X., W. Que, D. Fei, F. Shen, and Q. Guo. 2012. Ag nanoparticle/ZnO nanorods nanocomposites derived by a seed-mediated

method and their photocatalytic properties. *Journal of Alloys and Compounds* 524:13–21.

Yu, H.-F. 2007. Photocatalytic abilities of gel-derived P-doped TiO_2. *Journal of Physics and Chemistry of Solids* 68: 600–607.

Yu, H.-F., and H.-Y. Chou. 2013. Preparation and characterization of dispersive carbon-coupling ZnO photocatalysts. *Powder Technology* 233:201–207.

Zhang, S. C., and X. G. Li. 2003. Preparation of ZnO particles by precipitation transformation method and its inherent formation mechanisms. *Colloids and Surfaces A: Physicochemical and Engineering Aspects* 226:35–44.

Zheng, L., Y. Zheng, C. Chen, Y. Zhan, X. Lin, Q. Zheng, K. Wei, and J. Zhu. 2009. Network structured SnO_2/ZnO heterojunction nanocatalyst with high photocatalytic activity. *Inorganic Chemistry* 48:1819–1825.